

Sodium Sulfate Mixed with Rare Earth Sulfates(Ln=Y and Gd) and Silicon Dioxide as a Solid Electrolyte for a Sulfur Dioxide Detector

Nobuhito IMANAKA, Yasuo YAMAGUCHI, Gin-ya ADACHI,* and Jiro SHIOKAWA
Department of Applied Chemistry, Faculty of Engineering, Osaka University, Yamadaoka, Suita, Osaka 565
(Received May 14, 1984)

Sodium sulfate mixed with rare earth sulfates(Ln=Y and Gd) and silicon dioxide exhibits a Na_2SO_4-I-like phase as well as a small amount of silicon dioxide phase. The former phase is excellent in Na^+ ion conduction. The electrical conductivity of the Na_2SO_4-$Ln_2(SO_4)_3$-SiO_2(Ln=Y and Gd) systems is considerably higher than that of pure sodium sulfate. When the Na_2SO_4-$Ln_2(SO_4)_3$-SiO_2(Ln=Y and Gd) sample is applied as a solid electrolyte for a SO_2 gas concentration cell, the measured EMF is in good agreement with the calculated EMF for a SO_2 gas concentration range from 0.1% (1000 ppm) to 23%, and 0.32% (3200 ppm) to 10%, respectively.

Acid rain produced from the absorbtion of SO_2 and NO_2 in air is deteriorating the environment considerably in recent years. The control of the SO_2 and NO_2 in the exhausted gas and in the atmosphere is becoming a serious problem.

Alkali metal sulfates,[1-9] which are cation conductors at elevated temperature, have been applied as solid electrolytes for the SO_2 gas detector. Sodium sulfate holds the phase transformation from Na_2SO_4-III to Na_2SO_4-I.[10-26] The phase transformation, however, results in cracks in the electrolyte. The sulfate becomes soft at a temperature higher than approximately 1073 K. In addition, the electrical conductivity of Na_2SO_4 is appreciably lower than other Na^+ ion conductors such as NASICON.[27-32] Therefore, several attempts[33-37] to dope mono-, di-, or trivalent cations into sodium sulfate have been made to obtain higher electrical conductivity.

In our previous papers,[7-9,38] sodium vanadate and rare earth sulfates(Ln=Eu, Pr, and Y) have been doped in order to promote the oxidation from SO_2 to SO_3 and maintain the hig h conductive Na_2SO_4-I phase, and to increase the electrical conductivity.

In this investigation, silicon dioxide was added so as to obtain an effective network structure for Na^+ ion migration and in addition, to suppress the electrolyte becoming soft. Rare earth sulfates(Ln=Y and Gd) were also mixed to enhance the electrical conductivity. The suppression of the phase transformation from Na_2SO_4-I to Na_2SO_4-III was also attempted by mixing SiO_2 and $Ln_2(SO_4)_3$(Ln=Y and Gd) simultaneously with Na_2SO_4.

Experimental

Materials. Sodium sulfate(purity 99.99%) and silicon dioxide(purity 99.9%) were purchased from Wako Pure Chemical Industries Ltd. Yttrium(purity 99.9%) and gadlinium oxide(purity 99.99%) were bought from Shiga Rare Metal Industries Ltd. Yttrium and gadlinium sulfate were prepared by adding concd sulfuric acid into Y_2O_3 and Gd_2O_3, respectively. Sodium sulfate which is hygroscopic, and silicon dioxide were preheated before weighing. $Ln_2(SO_4)_3$ (Ln=Y and Gd) were also heated to eliminate the included water. Since $Ln_2(SO_4)_3$(Ln=Y and Gd) easily absorbs water, the real concentration of lanthanoid cation in the mixture was determined by the EDTA titration. Preheated materials were cooled in a desiccator, weighed, and mixed thoroughly in an agate mortar. Mixtures of Na_2SO_4-SiO_2 and Na_2SO_4-$Ln_2(SO_4)_3$-SiO_2(Ln=Y and Gd) were melted at 1473 K in air, then quenched in air. The resulting sample was pulverized in an agate ball, made into pellets under hydrostatic pressure (2.65×10^8 Pa) and then heated at 1073 K for 1 h in air.

Measurements. X-ray and thermal analyses were performed for the Na_2SO_4-SiO_2 and Na_2SO_4-$Ln_2(SO_4)_3$-SiO_2(Ln=Y and Gd) systems in order to investigate their phases and phase transformations using a Rigaku Rotaflex diffractometer equipped with a Cu target and a Rigaku Thermoflex, respectively. Electrical conductivities were measured by the complex impedance method[39] with a Hewlett Packard vector impedance meter 4800A. Electromotive force(EMF) measurements were carried out with a Takeda Riken Digital Multimeter TR-6841 by constructing the SO_2 gas concentration cell depicted in Fig. 1. Mixture gases of SO_2 ranging from 6% to 23% were prepared by controlling the SO_2 and the O_2

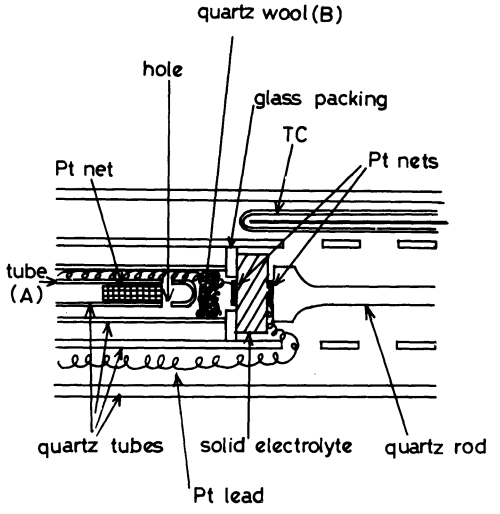

Fig. 1. The apparatus for the electromotive force (EMF) measurements.

gas flow volumes with self-made glass flow meters. The SO_2 gas concentration between 40 ppm and 11100 ppm was regulated by Standard Gas Generator(SGGU-711SD) from Standard Technology Co. The test SO_2 and O_2 gas mixture is introduced from the tube A depicted in Fig. 1. A Pt net is inserted so as to accelerate the oxidation of SO_2 to SO_3. The gas is led to the outer tube compartment through two small holes, and then reaches the electrolyte. The quartz wool is sacked in the place indicated by B shown in Fig. 1 in order to help to diffuse the gas uniformly and to avoid the occurrence of temperature gradient on the electrolyte surface. The ringed glass packing is fixed between the outer quartz tube of the test gas and the solid electrolyte by a spring loading a quartz rod so as to assure the separation of the test gas from the reference gas. The volume of the compartment for the reference SO_2 and O_2 gas mixture has been designed considerably larger compared with that for the test gas so that the SO_2-SO_3 equilibrium can be easily achieved.

Results and Discussion

Electrical Conductivity, Phases, and Thermal Properties. Na_2SO_4-SiO_2 Systems: Na_2SO_4-SiO_2 systems prepared are listed in Table 1 together with the results of X-ray and thermal analyses. All samples show the Na_2SO_4-III phase along with SiO_2. DTA curves also indicate a typical peak of the phase transformation from Na_2SO_4-III to Na_2SO_4-I at 513 K. Addition of silicon dioxide to sodium sulfate does not contribute to obtaining the Na_2SO_4-I-like phase which is excellent in the Na^+ ion conduction.

Electrical conductivity measurements for Na_2SO_4-SiO_2 systems are shown in Fig. 2. Mixing SiO_2 with Na_2SO_4 does not enhance the electrical conductivity. The discontinuity in the $\log(\sigma T)$-$1/T$ curve which is attributed to the III to I phase transformation, also exists for the Na_2SO_4-SiO_2 systems. The temperature at the break is about 513 K, which exactly coincides with the temperature obtained by the DTA measurements.

TABLE 1. THE PHASES AND THERMAL PROPERTIES OF Na_2SO_4-SiO_2

Sample No.	Na_2SO_4 (mol%)	SiO_2 (mol%)	Phases	DTA peak T/K
1	90	10	Na_2SO_4-III + SiO_2	513
2	70	30	Na_2SO_4-III + SiO_2	513
3	50	50	Na_2SO_4-III + SiO_2	513

The Na_2SO_4-SiO_2 systems, therefore, do not seem to be suitable for solid electrolytes because of their low electrical conductivities and because of the existence of the phase transformation from III to I.

Na_2SO_4-$Y_2(SO_4)_3$-SiO_2 Systems: The results of phase analyses and DTA measurements are presented in Table 2. X-Ray measurements indicate that a new phase, A, in which the peaks of Na_2SO_4-I-like phase are included, and a small amount of SiO_2 coexist. In sample No.1, some peaks of phase A split. Therefore, a symbol A′ is given to this phase instead of A. This sample(No.1) exhibits an endothermal peak with no gravimetric change at 593 K, showing that a phase transformation occurs. On the other hand, samples from No. 2 to 5 exhibit no phase transition.

Figure 3 illustrates the electrical conductivities results for Na_2SO_4-$Y_2(SO_4)_3$-SiO_2 systems. Sample No.1 exhibits relatively high conductivity. However, the discontinuity lies in the $\log(\sigma T)$ *vs.* $1/T$ curve approximately at 593 K. This temperature is identical with the result from DTA measurement. Similar $\log(\sigma T)$-$1/T$ curves were obtained for the samples of No, 2, 3, and 4. Their curves are nearly straight lines and their conductivities are about 20 times larger than that of Na_2SO_4 at 873 K. In the case of 14.8 mol% $Y_2(SO_4)_3$(No. 5), the electrical conductivity decreased. The cation vacancies are apt to form clusters which do not contribute to the cation conduction.

In the systems of Na_2SO_4-$Y_2(SO_4)_3$-SiO_2, the samples from No. 2 to 4 can be applied as solid electrolytes for a

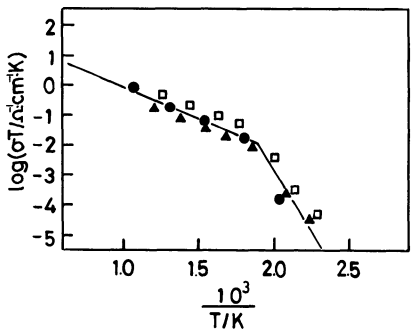

Fig. 2. Temperature dependences of electrical conductivities for the Na_2SO_4-SiO_2.
●: Na_2SO_4 : SiO_2 = 90 : 10,
□: Na_2SO_4 : SiO_2 = 70 : 30,
▲: Na_2SO_4 : SiO_2 = 50 : 50,
—: Na_2SO_4.

TABLE 2. THE PHASES AND THERMAL PROPERTIES OF Na_2SO_4-$Y_2(SO_4)_3$-SiO_2

Sample No.	Na_2SO_4 (mol%)	$Y_2(SO_4)_3$ (mol%)	SiO_2 (mol%)	Phases	DTA peak T/K
1	55.1	4.9	40.0	A′ + (small SiO_2)	593
2	52.2	7.7	40.1	A + (small SiO_2)	—
3	50.1	9.9	40.0	A + (small SiO_2)	—
4	48.1	11.8	40.1	A + (small SiO_2)	—
5	45.1	14.8	40.1	A + (small SiO_2)	—

A and A′: the phase which includes the peaks of Na_2SO_4-I-like phase.

SO_2 gas detector.

Na_2SO_4-$Gd_2(SO_4)_3$-SiO_2 Systems: The phases and thermal properties of Na_2SO_4-$Gd_2(SO_4)_3$-SiO_2 systems are tabulated in Table 3. The samples No. 1 to No. 4 exhibit a new phase α with a small amount of SiO_2. This phase is the phase where some peaks of phase A, are disappearing. The peaks of phase α' are slightly deviated from those of phase α toward low degree side except a peak at 31.6 degree. From thermal analyses, every sample exhibits no endo or exothermal peak on its DTA curve. The results of electrical conductivities for Na_2SO_4-$Gd_2(SO_4)_3$-SiO_2 systems are presented in Fig. 4. The electrical conductivities for the sample No. 1—3 show the highest values in the systems (at temperature higher than 781 K). In the case of 11.6mol% $Gd_2(SO_4)_3$, its conductivity decreased. This is because of the formation of cation vacancy clusters. When 17.2 mol% of $Gd_2(SO_4)_3$ is added(No. 5), the electrical conductivities becomes higher even at low temperatures. However, the bend in $\log(\sigma T)$ *vs.* $1/T$ curve appears at approximately 543 K.

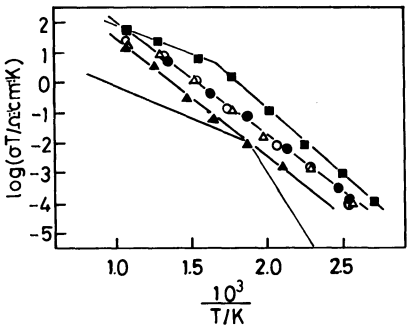

Fig. 3. Temperature dependences of electrical conductivities for the Na_2SO_4-$Y_2(SO_4)_3$-SiO_2.
-■-: $Na_2SO_4 : Y_2(SO_4)_3 : SiO_2 = 55.1 : 4.9 : 40.0$,
-○-: $Na_2SO_4 : Y_2(SO_4)_3 : SiO_2 = 52.2 : 7.7 : 40.1$,
-●-: $Na_2SO_4 : Y_2(SO_4)_3 : SiO_2 = 50.1 : 9.9 : 40.0$,
-△-: $Na_2SO_4 : Y_2(SO_4)_3 : SiO_2 = 48.1 : 11.8 : 40.1$,
-▲-: $Na_2SO_4 : Y_2(SO_4)_3 : SiO_2 = 45.1 : 14.8 : 40.1$,
——: Na_2SO_4.

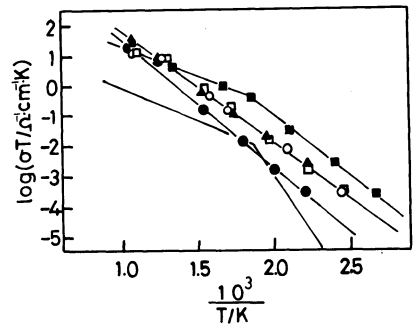

Fig. 4. Temperature dependences of electrical conductivities for the Na_2SO_4-$Gd_2(SO_4)_3$-SiO_2.
-□-: $Na_2SO_4 : Gd_2(SO_4)_3 : SiO_2 = 55.2 : 4.7 : 40.1$,
-○-: $Na_2SO_4 : Gd_2(SO_4)_3 : SiO_2 = 52.0 : 8.0 : 40.0$,
-▲-: $Na_2SO_4 : Gd_2(SO_4)_3 : SiO_2 = 51.0 : 8.2 : 40.8$,
-●-: $Na_2SO_4 : Gd_2(SO_4)_3 : SiO_2 = 48.2 : 11.6 : 40.2$,
-■-: $Na_2SO_4 : Gd_2(SO_4)_3 : SiO_2 = 43.8 : 17.2 : 39.0$,
——: Na_2SO_4.

Na₂SO₄-Gd₂(SO₄)₃-SiO₂ Systems: The phases and thermal properties of Na_2SO_4-$Gd_2(SO_4)_3$-SiO_2 systems are tabulated in Table 3. The samples No. 1 to No. 4 exhibit a new phase α with a small amount of SiO_2. This phase is the phase where some peaks of phase A, are disappearing. The peaks of phase α' are slightly deviated from those of phase α toward low degree side except a peak at 31.6 degree. From thermal analyses, every sample exhibits no endo or exothermal peak on its DTA curve. The results of electrical conductivities for Na_2SO_4-$Gd_2(SO_4)_3$-SiO_2 systems are presented in Fig. 4. The electrical conductivities for the sample No. 1—3 show the highest values in the systems (at temperature higher than 781 K). In the case of 11.6mol% $Gd_2(SO_4)_3$, its conductivity decreased. This is because of the formation of cation vacancy clusters. When 17.2 mol% of $Gd_2(SO_4)_3$ is added(No. 5), the electrical conductivities becomes higher even at low temperatures. However, the bend in $\log(\sigma T)$ *vs.* $1/T$ curve appears at approximately 543 K.

In the Na_2SO_4-$Gd_2(SO_4)_3$-SiO_2 systems, the samples No. 1—3 are good candidates for solid electrolytes.

EMF Measurements: EMF measurements with the appropriate sample of Na_2SO_4-$Y_2(SO_4)_3$-SiO_2 (50.1 : 9.9 : 40.0) are shown in Fig. 5. The measured EMF was in good agreement with the calculated EMF, with the initial SO_2 gas concentration between 0.1% (1000 ppm) and 23%. When the initial SO_2 gas concentration was less than 0.1%, the measured EMF becomes lower than the calculated EMF. Figure 6 presents the variation of the EMF with the pertinent sample of Na_2SO_4-$Gd_2(SO_4)_3$-SiO_2 (51.0:8.2:40.8). The measured EMF coincided with calculated EMF, with the initial SO_2 gas range from 0.32% (3200 ppm) to 10%. When the initial SO_2 gas content was smaller than 0.32%, the difference between the measured and the calculated EMF became larger. The reason that the measured

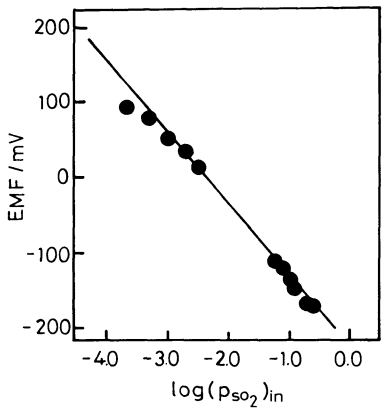

Fig. 5. Variation of the EMF for the concentration cell; $Pt|O_2(p_1'), SO_2(p_2')|Na_2SO_4$(9.9 mol% $Y_2(SO_4)_3$, 40.0 mol% SiO_2)$|O_2(p_1''), SO_2(p_2'')|Pt$, with $p_1''=0.996$ and $p_2''=0.004$ at 973 K.
—— is calculated EMF.[5]

Table 3. The phases and thermal properties of Na_2SO_4-$Gd_2(SO_4)_3$-SiO_2

Sample No.	Na_2SO_4 (mol%)	$Gd_2(SO_4)_3$ (mol%)	SiO_2 (mol%)	Phases	DTA peak T/K
1	55.2	4.7	40.1	α + (small SiO_2)	—
2	52.0	8.0	40.0	α + (small SiO_2)	—
3	51.0	8.2	40.8	α + (small SiO_2)	—
4	48.2	11.6	40.2	α + (small SiO_2)	—
5	43.8	17.2	39.0	α' + (small SiO_2)	—

α and α': the phase which includes the peaks of Na_2SO_4-I-like phase.

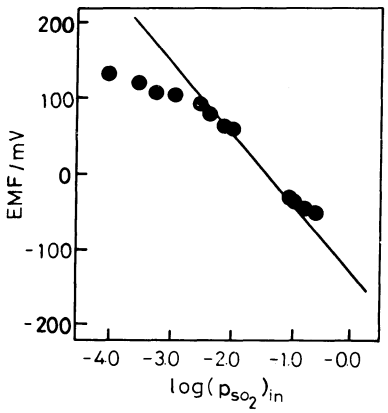

Fig. 6. Variation of the EMF for the concentration cell; Pt|$O_2(p_1')$, $SO_2(p_2')$|Na_2SO_4(8.2 mol% $Gd_2(SO_4)_3$, 40.8 mol% SiO_2)|$O_2(p_1'')$, $SO_2(p_2'')$|Pt, with $p_1''=0.966$ and $p_2''=0.034$ at 973 K.
—— is calculated EMF.[5]

and the calculated EMF does not coincide at relatively lower SO_2 gas concentration, may be predominantly accounted to the inadequate oxidation of SO_2 to SO_3.

In conclusion, sodium sulfate mixed with $Ln_2(SO_4)_3$(Ln=Y and Gd) and SiO_2 maintains relatively high electrical conductivities. When Na_2SO_4–$Ln_2(SO_4)_3$–SiO_2 (Ln=Y and Gd) are applied as solid electrolytes for a sulfur dioxide gas sensor, they can detect the SO_2 gas in the initial SO_2 gas concentration range from 0.1% to 23%, and 0.32% to 10%, respectively.

The present work was partially supported by a Grant-in-Aid for Developmental Scientific Research No. 57850250 from the Ministry of Education, Science and Culture.

References

1) L. G. Boxall and K. E. Johnson, *J. Electrochem. Soc.*, **118**, 885 (1971).
2) M. Gauthier and A. Chamberland, *J. Electrochem. Soc.*, **124**, 1579 (1977).
3) M. Gauthier, A. Chamberland, A Bélanger, and M. Poirier, *J. Electrochem. Soc.*, **124**, 1584 (1977).
4) M. Gauthier, R. Bellemare, and A. Bélanger, *J. Electrochem. Soc.*, **128**, 371 (1981).
5) K. T. Jacob and D. B. Rao, *J. Electrochem. Soc.*, **126**, 1842 (1979).
6) W. L. Worrell, Pro. the International Meeting on Chemical Sensors, Fukuoka, 332 (1983).
7) N. Imanaka, G. Adachi, and J. Shiokawa, *Chem. Lett.*, **1983**, 287.
8) N. Imanaka, G. Adachi, and J. Shiokawa, *Denki Kagaku*, **51**, 93 (1983).
9) N. Imanaka, G. Adachi, and J. Shiokawa, *Bull. Chem. Soc. Jpn.*, **57**, 687 (1984).
10) J. P. Coughlin, *J. Am. Chem. Soc.*, **77**, 868 (1955).
11) Y. A. Badr, F. El-Kabbany, and M. Tosson, *Phys. Status Solidi A*, **53**, K51 (1979).
12) F. El-Kabbany, Y. Badr, and M. Tosson, *Phys. Status Solidi A*, **63**, 699 (1981).
13) Q. R. Goyal, V. V. Deshpande, and M. D. Karkhanavala, *Indian J. Chem.*, **9**, 1006 (1971).
14) J. E. D. Davies and W. F. Sandford, *J. Chem. Soc., Dalton Trans.*, **1975**, 1912.
15) B. N. Mehrotra, Th. Hahn, H. Arnold, and W. Eysel, *Acta Crystallogr., Sect. A*, **31**, S79 (1975).
16) V. Amirthalingam, M. D. Karkhanavala, and U. R. K. Rao, *Acta Crystallogr., Sect. A*, **33**, 522 (1977).
17) C. A. Cody, L. Dicarlo, and R. K. Darlington, *J. Inorg. Nucl. Chem.*, **43**, 398 (1981).
18) E. L. Kreidl and Ivan Simon, *Nature*, **181**, 1529 (1958).
19) Y. Saito, K. Kobayashi, and T. Maruyama, *Thermochim. Acta*, **53**, 289 (1982).
20) F. C. Kracek, *J. Phys. Chem.*, **33**, 1281 (1929).
21) F. C. Kracek and R. E. Gibson, *J. Phys. Chem.*, **33**, 1304 (1929).
22) F. C. Kracek and R. E. Gibson, *J. Phys. Chem.*, **34**, 188 (1930).
23) F. C. Kracek and C. J. Ksanda, *J. Phys. Chem.*, **34** 1741 (1930).
24) G. E. Brodale and W. F. Giauque, *J. Phys. Chem.*, **76**, 737 (1972).
25) K. Kobayashi and Y Saito, *Thermochim. Acta*, **53**, 299 (1982).
26) Y. Saito, K. Kobayashi, and T. Maruyama, *Solid State Ionics*, (**1981**) 393.
27) J. P. Boilot, J. P. Salanié, G. Desplanches, and D. Le Potier, *Mater. Res. Bull.*, **14**, 1469 (1979).
28) U. von Alpen, M. F. Bell, and W. Wichelhaus, *Mater. Res. Bull.*, **14**, 1317 (1979).
29) J. B. Goodenough, H. Y-P. Hong, and J. A. Kafalas, *Mater. Res. Bull.*, **11**, 203 (1976).
30) T. Takahashi, K. Kuwabara, and M. Shibata, *Solid State Ionics*, **1**, 163 (1980).
31) W. Bogusz, F. Krok, and W. Jakubowski, *Solid State Ionics*, **2**, 171 (1981).
32) U. von Alpen, M. F. Bell, and H. H. Höfer, *Solid State Ionics*, **3/4**, 215 (1981).
33) H. H. Höfer, W. Eysel, and U. v. Alpen, *J. Solid State Chem.*, **36**, 365 (1981).
34) H. H. Höfer, W. Eysel, and U. v. Alpen, *Mater. Res. Bull.*, **13**, 265 (1978).
35) R. M. Mupray and E. A. Secco, *Can. J. Chem.*, **56**, 2616 (1978).
36) K. L. Keester, W. Eysel, and Th. Hahn, *Acta Crystallogr., Sect. A*, **31**, S79 (1975).
37) H. H. Höfer, U. v. Alpen, and W. Eysel, *Acta Crystallogr., Sect. A*, **34**, S358 (1978).
38) N. Imanaka, G. Adachi, and J. Shiokawa, *Can. J. Chem.*, **61**, 1557 (1983).
39) J. E. Bauerle, *J. Phys. Chem. Solids*, **30**, 2657 (1969).